ISSN 2176-5480

22nd International Congress of Mechanical Engineering (COBEM 2013)
November 3-7, 2013, Ribeirão Preto, SP, Brazil

ESTIMATING THE MASS CHARACTERISTICS OF A DUMBBELL AIR BEARING SATELLITE SIMULATOR

Alexandre Macedo de Oliveira
Hélio Koiti Kuga
Valdemir Carrara
National Institute for Space Research (INPE) - São José dos Campos - SP
alexandre@dem.inpe.br hkk@dem.inpe.br val@dem.inpe.br

Abstract. *Dumbbell air bearings provide a three degrees of freedom platform for tests of all components (hardware and software) of an attitude control system, including control algorithms. They are aimed at simulating the frictionless space environment. To validate the simulation environment, the accurate knowledge of the mass characteristics (moments of inertia and center of gravity) of the assembly is necessary. This characterization is very important, since a misalignment between this center and the air bearing rotation center causes undesirable torques on the platform, which can be higher than those disturbances normally found at the space environment, therefore invalidating the minimum-torque environment characteristics of the simulator. This work presents a comparison of two methods for estimating the mass characteristics of a three degrees of freedom dumbbell air bearing: extended kalman filtering and nonlinear least squares, by using embedded sensors in the platform. Almost all equipment used in this experiment are engineering models of flight devices and therefore offer the realism required for this experiment. This work suggests methods for the appropriate choice of the estimation algorithm suitable for different types of air bearings for space applications.*

Keywords: *air bearing, satellite simulator, inertial systems, estimation.*

1. INTRODUCTION

Air bearing tables have been used for test and verification of software and embedded electronic for at least 50 years since the beginning of the space race (Schwartz *et al.*, 2003). The idea behind an air bearing satellite simulator is to provide three-axis angular movement in a frictionless environment, similar to the outer space. It is known that this idealization is not valid since there is many disturbance torques on the system. Drag, bearing friction and gravity center offset are the major source of disturbance torques that must be modeled in order to validate the environment. They must be minimized until become compatible with the torque normally found in the space environment, ensuring the validity of simulators.

In the 1970s, research in air bearings were responsible for studies of internal energy dissipation effects in space platforms (sloshing, drive mechanisms and joints) because failures were detected in various missions. Although the technology has also been widely used by the Russians (Soviets) at the same time, little relevant information were found to complement the historical review from Schwartz *et al.* (2003).

The first step for develop a complete hardware-in-the-loop satellite attitude control system simulator is to accurately estimate the inertia matrix and the position of the center of gravity, using only the embedded equipment at the air bearing table, a gyroscope triad and a star sensor.

We will bring forward two well-known methods for estimating a dumbbell air bearing mass characteristics by means of extended kalman filtering and nonlinear least squares. Comparisons will be made, including a description of pros and cons of each of the methods.

2. THEORETICAL BASIS

This section starts with a brief description of the attitude kinematics and dynamics of a rigid body, and supplemented with a description of the two estimation algorithms used in this paper.

2.1 Attitude kinematics and dynamics

Attitude kinematics of a generic body can be described in different modes. Usually, Euler angles or quaternions are used. The use of quaternions is justified by computational facility, since trigonometric functions are avoided, circumventing computational problems like divisions by zero. By the other hand, it presents some difficulty for attitude estimation due to the lack of independence of the four quaternion components, wich are related by the constraint that the quaternion has unit module. This constraint results in the singularity of the covariance matrix of the quaternion state (Lefferts *et al.*, 1962). With this view, we will use Euler angles for attitude propagation.

The body attitude with respect to the inertial reference can be represented by three separate rotations that align the two distinct reference systems. In the LVLH (Local Vertical, Local Horizontal) system (East(X)-North(Y)-Up(Z), the motion

ISSN 2176-5480

around X-axis is called pitch (ϕ), around Y-axis is called roll (θ) and around Z-axis is called heading (ψ). The LVLH system will be considered inertial system in this paper. Hence, the rotation sequence used in this work for Euler angles is 3-2-1 (Hugues, 1986; Wertz, 1978), represented by the following transformation matrix $\mathbf{C_{br}}$:

$$\mathbf{C}_{br} = \begin{bmatrix} \cos\phi\cos\psi & \cos\phi\sin\psi & -\sin\phi \\ \sin\phi\sin\theta\cos\psi - \cos\phi\sin\psi & \sin\phi\sin\theta\sin\psi + \cos\phi\cos\psi & \sin\phi\cos\theta \\ \cos\phi\sin\theta\cos\psi + \sin\phi\sin\psi & \cos\phi\sin\theta\sin\psi - \sin\phi\cos\psi & \cos\phi\cos\theta \end{bmatrix}. \tag{1}$$

The set of kinematic equations are given by:

$$\begin{bmatrix} \dot{\phi} \\ \dot{\theta} \\ \dot{\psi} \end{bmatrix} = \begin{bmatrix} 1 & \sin\phi\tan\theta & \cos\phi\tan\theta \\ 0 & \cos\phi & -\sin\phi \\ 0 & \sin\phi/\cos\theta & \cos\phi/\cos\theta \end{bmatrix} \begin{bmatrix} \omega_x \\ \omega_y \\ \omega_z \end{bmatrix} \tag{2}$$

where ω_x, ω_y and ω_z are the angular velocity measured at the body reference system.

The attitude dynamics of a rigid body is defined by the angular momentum law with respect to an inertial frame:

$$\dot{\mathbf{h}} = \mathbf{T}, \tag{3}$$

where $\mathbf{h}$ is the angular momentum vector, defined as:

$$\mathbf{h} = \mathbf{I}\omega, \tag{4}$$

in which $\mathbf{I}$ is the body inertia matrix and ω is the body angular velocity vector. $\mathbf{T}$ is the sum of external torques, divided into environmental and control torques, defined by:

$$\mathbf{T} = \mathbf{T_{env}} + \mathbf{T_{con}} \tag{5}$$

When expressed in a frame attached to the body, the attitude dynamics of a rigid body is represented by:

$$\mathbf{I}\dot{\omega} + \omega \times \mathbf{I}\omega = \mathbf{T} \tag{6}$$

Thus, the rigid body dynamics is a nonlinear function described in terms of angular velocities and external torque:

$$\dot{\omega} = \mathbf{I^{-1}}[\mathbf{T} - \omega \times \mathbf{I}\omega]. \tag{7}$$

The torque caused by the displacement of the center of gravity $\mathbf{T_{CG}}$ is obtained by:

$$\mathbf{T_{CG}} = \mathbf{R_{CG}} \times \mathbf{P}, \tag{8}$$

where $\mathbf{R_{CG}}$ is the the center of gravity position vector of the bearing with respect with the bearing rotation center and $\mathbf{P}$ is the weight vector. It can be noted that the vector $\mathbf{R_{CG}}$ is measured in body system reference and the vector $\mathbf{P}$ is known in the topocentric system reference:

$$\mathbf{P} = \begin{bmatrix} 0 & 0 & -mg \end{bmatrix}^{\mathbf{T}}, \tag{9}$$

where m is the the total mass of the table ang g is the local gravity acceleration. As torque is applied to the rigid body, we need to transform its coordenates from the local reference system to the body reference system:

$$\mathbf{T_{CG}} = \mathbf{R_{CG}} \times \mathbf{C}_{br}\mathbf{P}, \tag{10}$$

where $\mathbf{C}_{br}$ is the rotation matrix defined in Equation 1.

2.2 Extended Kalman Filter

Kalman filter, in its standard form, is an optimal minimum variance estimator incorporating uncertainties in the dynamic and observation models. Unlike its linear version, the extended Kalman filter is not optimal due to truncation of higher order terms.

Extended Kalman Filter is an state estimation algorithm that, with some adjustments, can also be used for parameter estimation. Most references on the subject divides the algorithm into two phases: prediction and correction (Aguirre, 2007; Maybeck, 1979).

We define a generic system with input vector $\mathbf{u}$, the state vector $\mathbf{x}$ and measurement vector $\mathbf{y}$, described by:

ISSN 2176-5480

$$\dot{\mathbf{x}} = \mathbf{f}(\mathbf{x}, \mathbf{u}, t) + \mathbf{w_k} \tag{11}$$

$$\mathbf{y_{k+1}} = \mathbf{h_{k+1}}(\mathbf{x_{k+1}}) + \mathbf{v_{k+1}} \tag{12}$$

$\mathbf{F}$ and $\mathbf{H_k}$ are nonlinear functions linking the state vector $\mathbf{x}$ to the dynamic and observation models, respectively. The process noise and observation noise are represented by random variables $\mathbf{w_k} = \mathbf{N}(0, \mathbf{Q})$ and $\mathbf{v_k} = \mathbf{N}(0, \mathbf{R})$, Gaussian distributions with zero mean and covariance $\mathbf{Q}$ and $\mathbf{R}$, in this sequence. It can be noted that the system prediction is continuous and the observation is discrete.

For $\mathbf{x} \in \mathbf{R}$, the covariance matrix $\mathbf{P}$ has dimension $\mathbf{n} \times \mathbf{n}$ and is defined as:

$$\mathbf{P} = cov[\mathbf{x}] = E[(\mathbf{x} - E[\mathbf{x}])(\mathbf{x} - E[\mathbf{x}])^T] = E[\mathbf{x}\mathbf{x}^T] - E[\mathbf{x}]E[\mathbf{x}]^T, \tag{13}$$

where the function E $[\mathbf{x}]$ is the mathematical expectation.

The first phase of the EKF is based entirely on the dynamics of the system. Given the initial state vector $\mathbf{x_0}$ at time t_0, and knowing the input $\mathbf{u}$ applied over time, the system states can be propagated and therefore predicted in any time t_1, with $t_1 > t_0$. This propagation is therefore done via numerical integration of the equation (11) considering no uncertainty.

For the covariance prediction, we use continuous Ricatti equation that incorporates the uncertainty of each state equation of the model to the covariance matrix:

$$\dot{\mathbf{P}} = \mathbf{F}\mathbf{P} + \mathbf{P}\mathbf{F}^\mathbf{T} + \mathbf{G}\mathbf{Q}\mathbf{G}^\mathbf{T}, \tag{14}$$

where $\mathbf{G}$ is the association matrix between the process noise and covariance matrix. $\mathbf{F}$ is the Jacobian of $\mathbf{f}$, defined by:

$$\mathbf{F} = D\mathbf{f}(\mathbf{x}) = \begin{bmatrix} \frac{\partial f_1}{\partial x_1} & \cdots & \frac{\partial f_1}{\partial x_n} \\ \\ \frac{\partial f_n}{\partial x_1} & \cdots & \frac{\partial f_n}{\partial x_n} \end{bmatrix}_{n \times n}. \tag{15}$$

The correction process is done by comparing the obtained measurement from the predicted state $\bar{\mathbf{x}}_{\mathbf{k+1}}$ with the actual value of $\mathbf{y_{k+1}}$ obtained by the sensor at time t_1, with $t_1 > t_0$. The balance (weighing) between the predicted values and the values obtained by the sensors is given by the Kalman gain $\mathbf{K_{k+1}}$. Thus, the equations that summarize the correction process are:

$$\mathbf{K_{k+1}} = \bar{\mathbf{P}}_{\mathbf{k+1}}\mathbf{H}^\mathbf{T}_{\mathbf{k+1}}[\mathbf{H_{k+1}}\bar{\mathbf{P}}_{\mathbf{k+1}}\mathbf{H}^\mathbf{T}_{\mathbf{k+1}} + \mathbf{R_{k+1}}]^{-1} \tag{16}$$

$$\hat{\mathbf{P}}_{\mathbf{k+1}} = [\mathbf{I} - \mathbf{K_k}\mathbf{H_{k+1}}]\bar{\mathbf{P}}_{\mathbf{k+1}} \tag{17}$$

$$\mathbf{Res_{k+1}} = \mathbf{y_{k+1}} - \mathbf{h}(\bar{\mathbf{x}}_{\mathbf{k+1}}) \tag{18}$$

$$\hat{\mathbf{x}}_{\mathbf{k+1}} = \bar{\mathbf{x}}_{\mathbf{k+1}} + \mathbf{K_{k+1}}\mathbf{Res_{k+1}}, \tag{19}$$

where $\bar{\mathbf{P}}$ is the predicted covariance matrix and $\hat{\mathbf{P}}$ is the corrected covariance matrix.

The vector $\hat{\mathbf{x}}_{\mathbf{k+1}}$ is the best estimate for the state at time $\mathbf{k} + \mathbf{1}$. The residue $\mathbf{Res}$ is defined as the difference between the sensor measurement and the value of the nonlinear function $\mathbf{h}$ applied to $\bar{\mathbf{x}}_{\mathbf{k+1}}$. The matrix $\mathbf{H}$ is the Jacobian of $\mathbf{h}$, applied at the point $\bar{\mathbf{x}}_{\mathbf{k+1}}$, and defined by:

$$\mathbf{H} = D\mathbf{h}(\mathbf{x}) = \begin{bmatrix} \frac{\partial h_1}{\partial x_1} & \cdots & \frac{\partial h_1}{\partial x_n} \\ \\ \frac{\partial h_n}{\partial x_1} & \cdots & \frac{\partial h_n}{\partial x_n} \end{bmatrix}_{n \times n}. \tag{20}$$

With the already computed $\hat{\mathbf{x}}_{\mathbf{k+1}}$ and $\hat{\mathbf{P}}_{\mathbf{k+1}}$ the algorithm is fed back, restarting the prediction and correction.

2.3 Nonlinear least squares

We assume the following continuous-discrete dynamic system:

$$\dot{\mathbf{x}} = \mathbf{f}(\mathbf{x}, \mathbf{u}, t) \tag{21}$$

$$\mathbf{y_k} = \mathbf{h_k}(\mathbf{x_k}) + \mathbf{v_k}, \tag{22}$$

Unline the EKF, the system dynamics is considered perfect, and therefore, there is no uncertainty related to the system model, in the least squares algorithm. For the least-squares algorithm, unlike the EKF, the dynamics of the system is considered perfect, and therefore, there is no uncertainty related to the system model.

ISSN 2176-5480

The nonlinear least squares estimator, on its discrete form, is responsible for minimizing a function of the squared residuals (Gelb, 2001):

$$\mathbf{L_k} = \sum_{\mathbf{i=1}}^{\mathbf{k}} (\mathbf{y_i} - \mathbf{h_i}(\mathbf{x_i}))^{\mathbf{T}} (\mathbf{y_i} - \mathbf{h_i}(\mathbf{x_i})), \tag{23}$$

where $\mathbf{y_i}$ is the vector of observations and $\mathbf{h_i}$ is a function that associates the observations to the model state vector $\mathbf{x_i}$. It is considered that the input vector $\mathbf{u}$ is known throughout the process. Thus, the estimation problem comes down to finding the vector of initial conditions $\mathbf{x_0}$ to minimize cost index $\mathbf{L_k}$. For this it is necessary to find the solution to the following family of differential equations:

$$\frac{\partial \mathbf{L_k}}{\partial \mathbf{x_{0_k}}} = \mathbf{0}. \tag{24}$$

We use the transition matrix $\mathbf{\Phi_k}$ to reference all state vectors $\mathbf{x_k}$ depending on the initial state vector $\mathbf{x_{0_k}}$. The algorithm for nonlinear least squares is iterative and refines the variations in the states and not the states themselves. The following deviations are defined:

$$\delta \bar{\mathbf{x}}_\mathbf{i} = \hat{\mathbf{x}}_\mathbf{i} - \hat{\mathbf{x}}_\mathbf{0} \tag{25}$$

$$\delta \hat{\mathbf{x}}_\mathbf{i} = \hat{\mathbf{x}}_\mathbf{i} - \hat{\mathbf{x}}_{\mathbf{i-1}}, \tag{26}$$

where $\delta \bar{\mathbf{x}}_i$ represents the deviation from the initial state and $\delta \hat{\mathbf{x}}_i$ represents the deviation from the previous state. The residue $\delta \mathbf{y}$ is defined as an array of m measurements obtained at each time t_n:

$$\delta \mathbf{y} = \begin{bmatrix} \mathbf{y}_{t_1} - \mathbf{h_{t_1}}(\hat{\mathbf{x}}_{t_1}) \\ \mathbf{y}_{t_2} - \mathbf{h_{t_2}}(\hat{\mathbf{x}}_{t_2}) \\ \vdots \\ \mathbf{y}_{t_n} - \mathbf{h_{t_n}}(\hat{\mathbf{x}}_{t_n}) \end{bmatrix} . \tag{27}$$

$\mathbf{H}$ is defined as the same form as described in Equation 20:

$$\mathbf{H} = \begin{bmatrix} \mathbf{H_1} \\ \mathbf{H_2} \\ \vdots \\ \mathbf{H_n} \end{bmatrix} = \begin{bmatrix} \mathbf{H}_{t_1} \mathbf{\Phi}_{t_1,t_0} \\ \mathbf{H}_{t_2} \mathbf{\Phi}_{t_2,t_0} \\ \vdots \\ \mathbf{H}_{t_n} \mathbf{\Phi}_{t_n,t_0} \end{bmatrix} , \tag{28}$$

where the matrix $\mathbf{\Phi}_{t_n,t_0}$ is found by integrating the state transition equation:

$$\dot{\mathbf{\Phi}} = \mathbf{F}\mathbf{\Phi}, \tag{29}$$

with initial condition Φ_0 being the identity matrix of equal order to the number of states to be estimated. After composing the matrices $\mathbf{H}$ and $\delta \mathbf{y}$, we execute the batch algorithm (Kuga, 2005):

$$\hat{\mathbf{P}}_\mathbf{i} = (\bar{\mathbf{P}}_\mathbf{0}^{-\mathbf{1}} + \mathbf{H}^\mathbf{T} \mathbf{R}^{-\mathbf{1}} \mathbf{H})^{-\mathbf{1}} \tag{30}$$

$$\delta \hat{\mathbf{x}}_\mathbf{i} = \hat{\mathbf{P}}_\mathbf{i} (\bar{\mathbf{P}}_\mathbf{0}^{-\mathbf{1}} \delta \bar{\mathbf{x}}_{\mathbf{i-1}} + \mathbf{H}^\mathbf{T} \mathbf{R}^{-\mathbf{1}} \delta \mathbf{y}). \tag{31}$$

Typically the iterations continue until convergence is reached. Basically, the criterion used to terminate the algorithm consists in checking when the deviation becomes sufficiently small. The final solution to the state of each iteration will be (Kuga, 2005):

$$\hat{\mathbf{x}}_\mathbf{i} = \hat{\mathbf{x}}_{\mathbf{i-1}} + \delta \hat{\mathbf{x}}_\mathbf{i}, \tag{32}$$

and covariance $\hat{\mathbf{P}}_\mathbf{i}$. The presented algorithm is known as batch least squares (BLS), since all the data are processed at once by the estimator. A variation of the BLS is the recursive least squares, where the data are processed one by one.

Using the recursive algorithm for nonlinear least squares is not advised, since numerical integration errors can hinder the process of refinement and convergence of the estimator.

ISSN 2176-5480

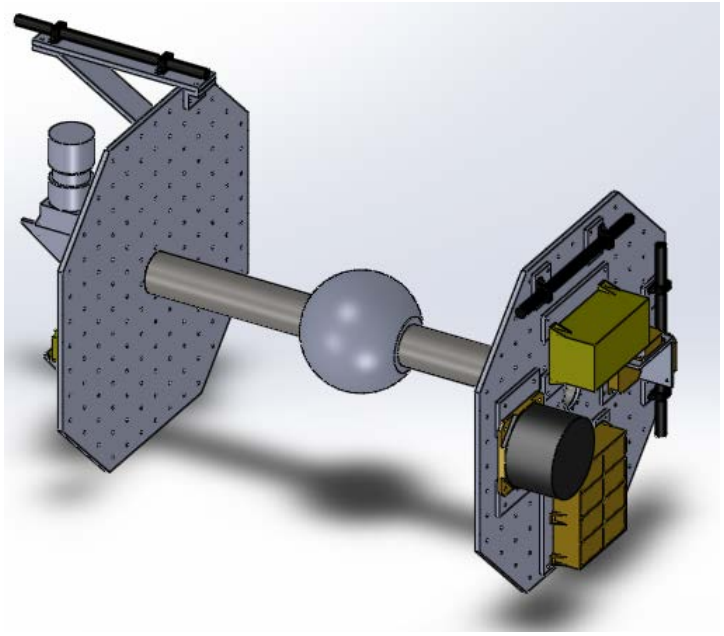

Figure 1. Dumbbell air bearing CAD model approach.

Table 1. Dumbell air bearing mass characteristics.

Inertia matrix ($kg.m^2$)	$\mathbf{I} = \begin{bmatrix} 3 & 0.1 & 0.1 \\ 0.1 & 12 & 0.1 \\ 0.1 & 0.1 & 13 \end{bmatrix}$
Gravity center position (m)	$\mathbf{R} = \begin{bmatrix} 10^{-6} & 10^{-6} & -10^{-6} \end{bmatrix}$

3. Results

A CAD model of the dumbbell air bearing used in this experiment can be seen in Fig. 1. All embedded equipment were draw with same dimensions, mass and center-of-mass according to each mechanical interface document, including fixing supports. Total mass is 72 kg and local gravity is 9.780327 m/s^2.

Table 1 shows the CAD computed inertia matrix and center of gravity position. A simulation of kinematics and dynamics will be performed with these information.

The state vector to be estimated $\mathbf{x}$ is:

$$\mathbf{x} = [\ \phi\ \theta\ \psi\ \omega_x\ \omega_y\ \omega_z\ I_{xx}\ I_{yy}\ I_{zz}\ I_{xy}\ I_{xz}\ I_{yz}\ mgR_x\ mgR_y\ mgR_z\ ]^T. \tag{33}$$

Table 2 shows the initial conditions for the EKF estimator. It can be observed that the uncertainty to the model is only added to the Euler Equations. Kinematics propagation model is considered perfect for this case.

Figure 2 shows four graphics of the attitude dynamic simulation. Both the quaternion and euler angles propagation are shown, wich represent the same information in two different modes. The table angular velocity is also presented in Figure 2.

Table 2. Initializing data for EKF.

Variables	Values
$[\ \phi\ \theta\ \psi\ ]$	$[\ 0\ 0\ 0\ ]\ rad$
$[\ \omega_x\ \omega_y\ \omega_z\ ]$	$[\ 0\ 0\ 0.2618\ ]\ rad/s$
$[\ Ixx\ Iyy\ Izz\ Ixy\ Ixz\ Iyz\ ]$	$[\ 3.0\ 11.5\ 12.5\ 0\ 0\ 0\ ]\ kg.m^2$
$[\ R_x\ R_y\ R_z\ ]$	$[\ 0\ 0\ 0\ ]\ m$
$diag(\sigma(\mathbf{x}))$	$[\ 1\ 1\ 1\ 1\ 1\ 1\ 2\ 2\ 1\ 1\ 1\ 0.01\ 0.01\ 0.01\ ]$
$diag(\mathbf{R})$	$[\ 8.72\times10^{-5}\ 8.72\times10^{-5}\ 8.72\times10^{-5}\ 1.92\times10^{-4}\ 1.92\times10^{-4}\ 1.92\times10^{-4}\ ]$
$diag(\mathbf{Q})$	$[\ 0\ 0\ 0\ 10^{-9}\ 10^{-9}\ 10^{-9}\ 0\ 0\ 0\ 0\ 0\ 0\ 10^{-14}\ 10^{-14}\ 10^{-14}\ ]$

Figures 3 and 4 show the estimation process during time. In blue, the state estimated value is observed. In green and

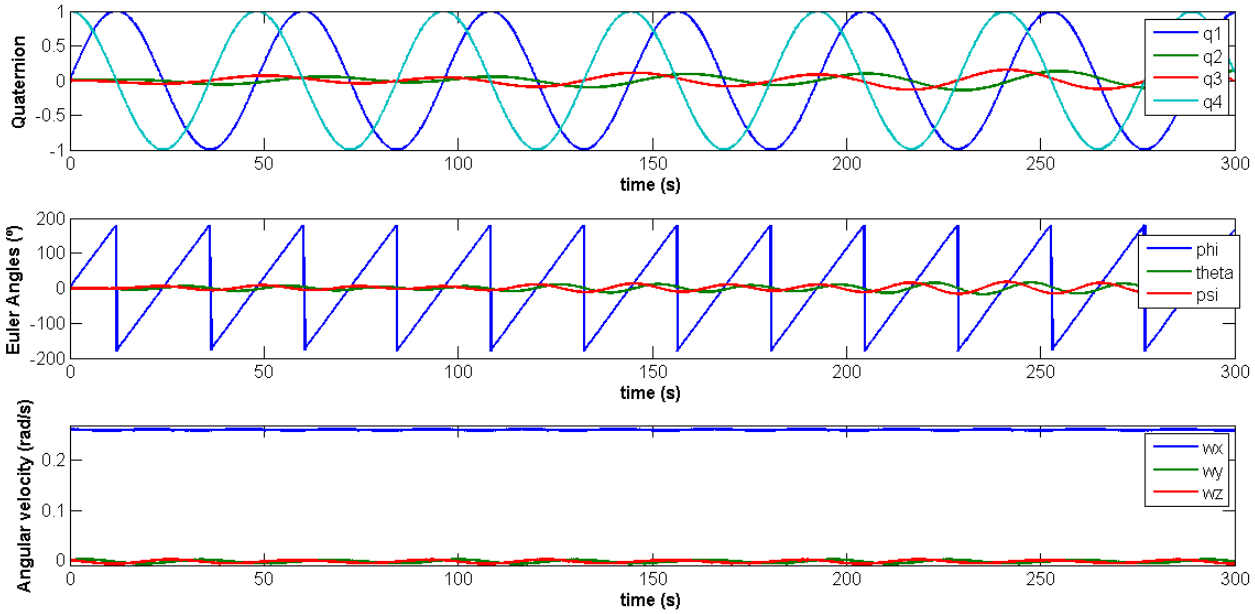

Figure 2. Kinematic and dynamic simulation of the air bearing table.

red we observe the estimated value added and subtracted from the standard deviation.

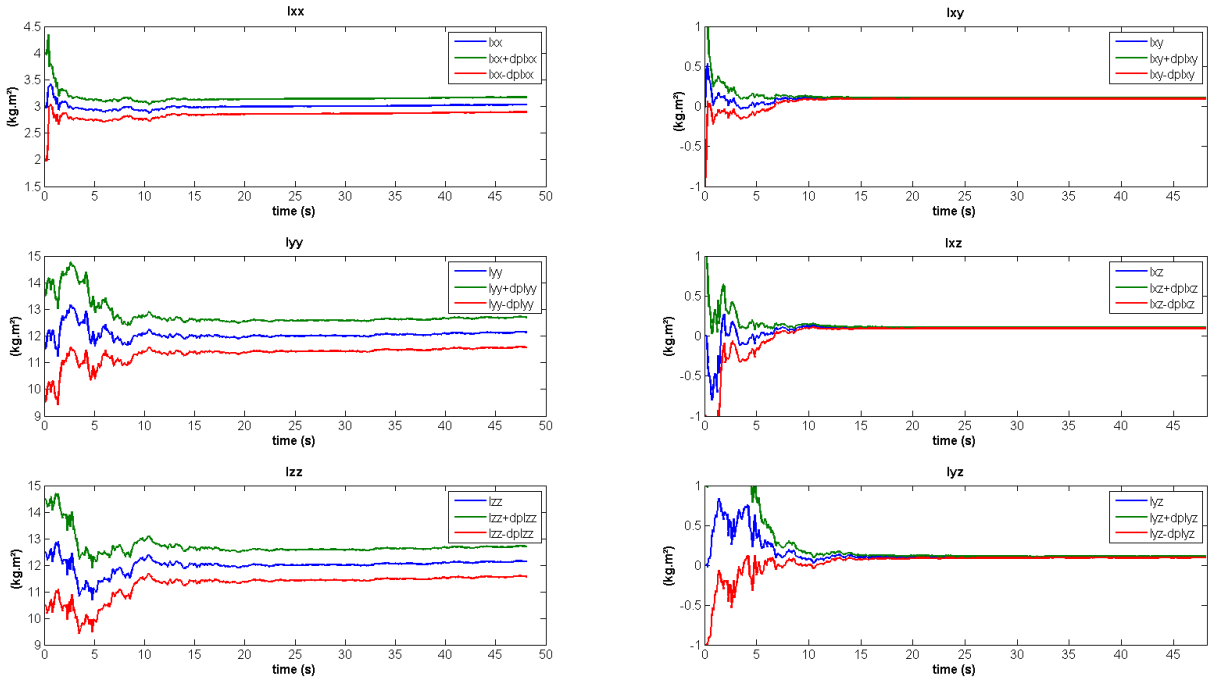

Figure 3. Estimated moments of inertia.

Table 3 shows the final estimated values for states, including each final standard deviation. We can see that the mean value is very close to the expected values of simulation.

The results obtained by the nonlinear least square method are presented in sequence, Table 4 shows the initial condition for the algorithm, while Figure 5 shows the behavior of the angular velocities residue in three different iterations.

The convergence of the least squares algorithm is proven when the residue tend to zero, maintaining a noisy pattern with the order of the uncertainty associated with the observations. Another important factor is the increment in the estimated values for the states, represented by the vector $\mathbf{\Delta x}$, which fall to a predefined limit.

If the increment of all states enter into the pre-established limits, the algorithm ends as expected and the last iteration provide the values of the estimated parameters. Table 5 shows the final result of the estimation process for the inertia matrix and gravity center position of the body.

ISSN 2176-5480

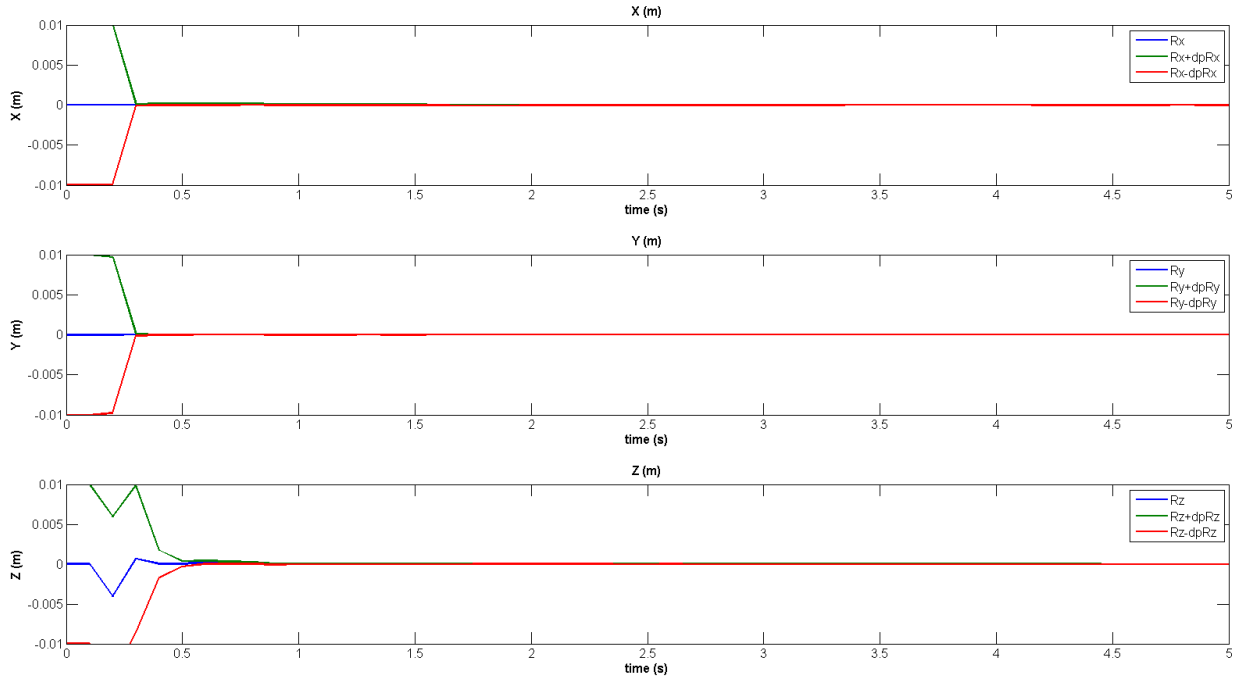

Figure 4. Estimated position of gravity center.

Table 3. Air bearing estimated mass characteristics using EKF.

Results	Values
Inertia matrix ($km.m^2$)	$\mathbf{I} = \begin{bmatrix} 3.0326 & 0.1011 & 0.1012 \\ 0.1011 & 12.1381 & 0.1012 \\ 0.1012 & 0.1012 & 12.1376 \end{bmatrix}$
Gravity center position (m)	$\mathbf{R_{CG}} = \begin{bmatrix} 1.027 \times 10^{-6} \\ 0.974 \times 10^{-6} \\ -1.000 \times 10^{-6} \end{bmatrix}$
Standard deviation matrix ($kg * m^2$)	$\sigma(\mathbf{I}) = \begin{bmatrix} 0.1398 & 0.0048 & 0.0048 \\ 0.0048 & 0.5641 & 0.0078 \\ 0.0048 & 0.0078 & 0.5644 \end{bmatrix}$
Standard deviation matrix (m)	$\sigma(\mathbf{R_{CG}}) = \begin{bmatrix} 2.676 \times 10^{-7} \\ 1.805 \times 10^{-7} \\ 2.395 \times 10^{-7} \end{bmatrix}$

Table 4. Initial conditions for the nonlinear least square estimator.

Variables	Values
$[\ \phi\ \theta\ \psi\ ]$	$[\ 0\ 0\ 0\ ]\ rad$
$[\ \omega_x\ \omega_y\ \omega_z\ ]$	$[\ 0\ 0\ 0.2618\ ]\ rad/s$
$[\ Ixx\ Iyy\ Izz\ Ixy\ Ixz\ Iyz\ ]$	$[\ 3.0\ 11.5\ 12.5\ 0\ 0\ 0\ ]\ kg.m^2$
$[\ R_x\ R_y\ R_z\ ]$	$[\ 0\ 0\ 0\ ]\ m$
$diag(\sigma(\mathbf{x}))$	$[\ 1\ 1\ 1\ 1\ 1\ 1\ 2\ 2\ 1\ 1\ 1\ 0.01\ 0.01\ 0.01\ ]$
$diag(\mathbf{R})$	$[\ 8.72 \times 10^{-5}\ 8.72 \times 10^{-5}\ 8.72 \times 10^{-5}\ 1.92 \times 10^{-4}\ 1.92 \times 10^{-4}\ 1.92 \times 10^{-4}\ ]$

4. Conclusions

We observe that both estimation algorithms had satisfactory behavior and accomplished good results for the inertia matrix and center-of-mass position. By the comparison of algorithms, we note that the EKF obtained a better result when compared with nonlinear least squares for this case. This fact is explained by comparing the robustness of the algorithms. The concept of robustness of an estimator is closely related to its ease of obtaining the convergence of states, using a larger number of different initial conditions. If we vary the initial conditions, heading to worst initial guess, the EKF

ISSN 2176-5480

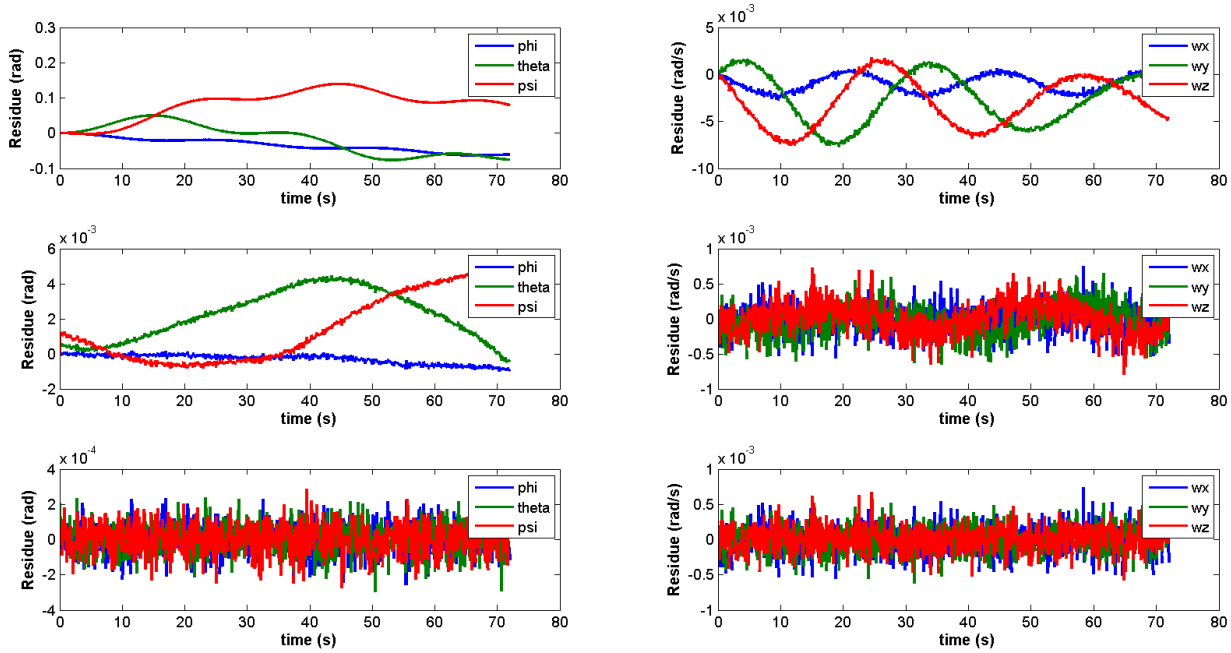

Figure 5. Angular position (left) and angular velocity (right) residue of nonlinear least square estimator for first, third and fifth estimation cycle.

Table 5. Estimated mass characteristics using nonlinear least square algorithm.

Results	**Values**
Inertia Matrix ($km.m^2$)	$\mathbf{I} = \begin{bmatrix} 3.0073 & 0.1020 & 0.1016 \\ 0.1020 & 12.1728 & 0.1018 \\ 0.1016 & 0.1018 & 12.1505 \end{bmatrix}$
Standard deviation matrix ($kg * m^2$)	$\sigma(\mathbf{I}) = \begin{bmatrix} 0.3333 & 0.0111 & 0.0111 \\ 0.0111 & 1.3333 & 0.0112 \\ 0.0111 & 0.0112 & 1.3329 \end{bmatrix}$
CG Position (m)	$\mathbf{R} = \begin{bmatrix} 1.0163 \times 10^{-6} \\ 1.0150 \times 10^{-6} \\ -1.0141 \times 10^{-6} \end{bmatrix}$
Standard deviation matrix (m)	$\sigma(\mathbf{R}) = \begin{bmatrix} 1.1103 \times 10^{-7} \\ 1.1115 \times 10^{-7} \\ 1.1092 \times 10^{-7} \end{bmatrix}$

will continue to accomplish convergence. The same does not happen with the nonlinear least square filter because this algorithm is much more sensitive to the nonlinearities of the problem. Therefore, choosing good initial conditions for attitude dynamics and parameter estimation problems is very important.

Another substantial fact is in the system nonlinear behavior. For obtaining a better estimation of all principal moments of inertia, it is suggested that all axis are fully excited. In this problem, just the X-axis were fully excited. The small angular movement at the other two is caused by coning motion. This fact can be confirmed by comparing the final standard deviation of the $\mathbf{I_{xx}}$ with the other ones $\mathbf{I_{yy}}$ and $\mathbf{I_{zz}}$. For both estimators, the lowest standard deviation was obtained for the X-axis, instead of the Y-axis or the Z-axis. Hence, for nonlinear problems, it is suggested that the set of measurements excite all system modes. For dumbbell air bearing tables, the Y-axis can not be fully excited and the estimation process may be worst for the parameters that are more sensitive with the Y-axis rotation. This is more intensified in the nonlinear least square because the algorithm itself is more susceptible to a bed set of measurements. Also, we can base the commentary of the last paragraph by analysing the EKF result. It is obviously noted that the states $\mathbf{I_{yy}}$, $\mathbf{I_{zz}}$ and $\mathbf{I_{yz}}$ does not have the same observability level of the states $\mathbf{I_{xx}}$, $\mathbf{I_{xy}}$ and $\mathbf{I_{xz}}$, due to less sensitivity of these states among the set of measurements.

By choosing a more precise initial conditions for the parameters, the nonlinear least square algorithm must return more reliable values, which represent more effectively the nature of the nonlinear problem. The combination of both estimation methods could ensure a more trustful result.

ISSN 2176-5480

5. ACKNOWLEDGEMENTS

Authors acknowledge funding by SIA project and INPE.

6. REFERENCES

Aguirre, L.A., 2007. *Introdução a Identificação de Sistemas*. Ed. UFMG, MG, Brasil, 3rd edition. 730 p.

Gelb, A., 2001. *Applied Optimal Estimation*. Ed. MIT Press, MA, USA. 384 p.

Hugues, P.C., 1986. *Spacecraft Attitude Dynamics*. Ed. Dover Publications, NY, USA. 570 p.

Kuga, H.K., 2005. "Noções práticas de técnicas de estimação". Technical report.

Lefferts, E.J., Markley, F.L. and Shuster, M.D., 1962. "Kalman filtering for spacecraft attitude estimation". Vol. 5, No. 5, pp. 417–429.

Maybeck, P.S., 1979. *Stochastic Models, Estimation, and Control*, Vol. 1. Ed. New York: Academic Press, New York, USA. 423 p.

Schwartz, J.L., Peck, M.A. and Hall, C.D., 2003. "Historical survey of air-bearing spacecraft simulators". *Journal of Guidance, Control, and Dynamics*, Vol. 26, No. 4, pp. 513–522.

Wertz, J.R., 1978. *Spacecraft Attitude Determination and Control*. Ed. Kluwer Academic Publishers, Dordrecht, The Netherlands. 860 p.

7. RESPONSIBILITY NOTICE

The author are the only responsible for the printed material included in this paper.